ELSEVIER

Ceramics International 29 (2003) 933–937

CERAMICS INTERNATIONAL

www.elsevier.com/locate/ceramint

Study on the phase-separated opaque glaze in ancient China from Qionglai kiln

Weidong Li*, Jiazhi Li, Jun Wu, Jingkun Guo

Shanghai Institute of Ceramics, Chinese Academy of Sciences, Shanghai 200050, China

Received 2 January 2003; received in revised form 20 January 2003; accepted 10 February 2003

Abstract

Qionglai kiln is a famous folk kiln site in China. Six pieces of opaque green-glazed porcelain shards with mild gloss and jade-like feel fired in the Tang dynasty (618–907 A.D.), were adopted as test samples. The correlation among composition, microstructure, firing technique and glaze appearance has been investigated by means of energy-dispersive X-ray fluorescence, field emission electron microscopy, direct transmission electron microscopy, X-ray diffraction and refiring experiment. The study has demonstrated that the opaque green glazes from Qionglai kiln site are high-temperature calcia–magnesia–silicate glazes and typical of phase-separated glazes. The liquid–liquid immiscibility structure plays a key role for the artistic appearance of the glazes.

Keywords: B. Microstructure-final; C. Color; D. Glass

1. Introduction

Qionglai kiln, a famous folk kiln located at Qionglai county in Sichuan province, southwest of China, bears a unique national style and specific local features. Qionglai kiln was established in the South dynasty (420–589 A.D.), flourished in the Tang dynasty (618–907 A.D), and declined in the intermediate and late stages of the Southern Song dynasty (1127–1279 A.D) [1,2]. Qionglai kiln series includes Wayaoshan kiln site, Jianzishan kiln site, Dayucun kiln site and Shifangtang kiln site, among which Shifangtang kiln is the largest one with typical features of the Tang dynasty [2]. The main products of Qionglai kiln are ornamental and household wares, among which a kind of opaque green-glazed wares turn out striking mild gloss and jade-like feel. Six pieces of such opaque green-glazed shards, numbered as Q1–Q6, excavated from Shifangtang kiln site in the Tang dynasty stratum were selected as test samples in order to further investigate the correlation among composition, microstructure, firing technique and glaze appearance.

2. Experimental

Glaze microstructures were studied using field emission electron microscopy (JSM-6700F, Japan). FESEM samples were obtained by etching polished cross sections of glazes in 1 wt.% HF at room temperature. The chemical compositions of the bodies and glazes were examined by energy-dispersive X-ray fluorescence (DX-95, USA). Phase compositions were determined by transmission electron microscope equipped with EDS and SAD (JEM-2 100, Japan). TEM powder samples were acquired by scrapping glaze surface with a glass cutter. X-ray diffraction (D/max 2550 V, Japan) using Cu-K_α radiation was employed to identify the crystalline phases in glaze. Physical properties of the bodies in terms of water absorption, porosity and bulk density were measured by Archimedes' principle. Refiring experiments were carried out in a gradient tube furnace.

3. Results and discussion

3.1. Chemical compositions and characteristics of the shards

As shown in Table 1, the glazes are attributed to high-temperature calcia–magnesia–silicate glazes with the

* Corresponding author. Tel.: +86-21-52412373; fax: +86-21-52413903.

E-mail address: liwd@mail.sic.ac.cn (W. Li).

0272-8842/03/$30.00
doi:10.1016/S0272-8842(03)00048-8

Table 1
Chemical compositions and characteristics of the shards (wt%)

No.		K_2O	Na_2O	CaO	MgO	Fe_2O_3	TiO_2	Al_2O_3	P_2O_5	SiO_2
Q1	B	1.62	0.37	0.32	1.63	3.52	1.03	14.49	0.29	76.59
	G	1.05	0.29	19.46	5.41	1.62	0.60	9.26	1.22	60.80
	C	Grayish green opaque glaze, gray body								
Q2	B	2.18	0.50	0.48	3.92	3.41	1.13	15.59	0.32	72.32
	G	1.34	0.23	18.80	5.86	1.83	0.50	7.87	1.44	61.77
	C	Light yellowish green opaque glaze, yellowish gray body								
Q3	B	1.53	0.27	0.33	1.93	2.59	1.07	15.40	0.27	76.37
	G	1.20	0.32	16.94	6.88	2.24	0.58	9.28	1.45	60.78
	C	Yellowish green opaque glaze, gray body								
Q4	B	1.92	0.73	0.30	2.79	2.64	1.00	15.48	0.27	74.71
	G	2.64	0.25	14.89	4.31	1.64	0.47	9.92	1.16	63.85
	C	Greenish white opaque glaze, yellowish gray body								
Q5	B	1.76	0.45	0.35	2.75	3.12	1.07	15.31	0.29	75.02
	G	1.19	0.19	17.71	5.33	1.53	0.51	8.77	1.42	62.53
	C	Bluish green opaque glaze, light gray body								
Q6	B	2.03	1.07	0.34	2.31	2.63	1.00	14.75	0.29	75.43
	G	2.04	0.32	19.22	4.24	1.66	0.76	9.07	2.00	60.03
	C	Dark green opaque glaze, light gray body								

unusual high calcia and magnesia contents. The glaze compositions could be written in a seger formula as follows.

$$\left.\begin{matrix}0.03\sim0.08\mathrm{KNaO}\\0.61\sim0.7\mathrm{lCaO}\\0.22\sim0.35\mathrm{MgO}\\0.02\sim0.03\mathrm{Fe_2O_3}\end{matrix}\right\}0.15\sim0.24\mathrm{Al_2O_3}\left\{\begin{matrix}2.02\sim2.57\mathrm{SiO_2}\\0.02\sim0.03\mathrm{P_2O_5}\\0.01\sim0.14\mathrm{TiO_2}\end{matrix}\right. \quad (1)$$

While the body compositions have relatively high silica and low alumina concentrations with some impurity iron oxide and titania. Body formula is as follows.

$$\left.\begin{matrix}0.13\sim0.23\mathrm{KNaO}\\0.03\sim0.05\mathrm{CaO}\\0.29\sim0.56\ \mathrm{MgO}\end{matrix}\right\}\left.\begin{matrix}0.88\sim6.90\mathrm{Al_2O_3}\\0.10\sim0.12\mathrm{Fe_2O_3}\end{matrix}\right\}\left.\begin{matrix}6.90\sim7.59\mathrm{SiO_2}\\0.01\mathrm{P_2O_5}\\0.07\sim0.08\mathrm{TiO_2}\end{matrix}\right\} \quad (2)$$

The glaze color or body color variations come from the fluctuation of firing conditions such as firing temperature, time and atmosphere in the hill-climbing dragonkilns with wood as fuel. In general, for the labile iron ions, a reduction–oxidation equilibrium exists as determined by glaze melt status and kiln atmosphere.

3.2. Physical properties of the bodies

The bodies are quite porous with white quartz particles trapped and the fracture surfaces are coarse and matte like stonewares, showing various degrees of underfiring. Water absorption, porosity and bulk density of the bodies were listed in Table 2.

Table 2
Physical properties of the bodies

No.	Bulk density (g/cm^3)	Water absorption (%)	Apparent porosity (%)
Q1	2.06	3.5	8.4
Q2	1.78	11.9	26.9
Q6	2.01	5.5	12.7

3.3. Microstructure of the glazes and the cause for liquid–liquid phase separation

XRD pattern of glaze Q6 (Fig. 1) shows the presence of a little unmelted quartz crystal in the glaze, and the most part of the glaze is an amorphous phase.

Both FESEM and TEM (Figs. 2 and 3) demonstrate that the glazes are of an evenly dispersed submicron droplet phase-separated structure, in which the equivalent diameter of the droplets falls into the range of 0.1–0.4 μm. In the liquid–liquid immiscibility structure, the isolated droplets are rich in SiO_2 and the matrix is rich in oxides of Ca, Mg, P, Ti and Fe (Fig. 3). SAD graphs of the droplets and matrices present dispersive rings attributed to amorphous phases (Fig. 3).

Based on the ideas of crystallochemistry, liquid–liquid immiscibility arises from competition between the cations to surround themselves with a minimum energy oxygen configuration, subject to limitations of the network-forming tendency of silica. The greater the difference in ionic field strength between a silicon ion with an oxygen ion and a modifying ion with an oxygen ion, the stronger the tendency to immiscibility.

SiO_2–CaO system contains a stable immiscibility gap between liquids containing about 70 and 97 mol.% SiO_2 at 1700 °C, addition of Al_2O_3 lowers the immiscibility temperature for liquid–liquid phase separation as the region of immiscibility is extended into the ternary field [3], which can be of quite considerable practical importance. Hence phase separation in the glazes of this work should be primarily determined by the strong immiscibility tendency between SiO_2 and RO (CaO, MgO). Considering the higher polarizability of nonbridging oxygen atoms compared to that of bridging ones, other modifiers such as phosphorous, titanium and iron ions locate preferably in the phase enriched by CaO and MgO oxides with a large number of nonbridging oxygen atoms, consequently favoring phase separation. Al_2O_3 acts as a homogenizing agent in such a low alkali system, which can severely decrease the immiscibility temperature to below the liquidus, accordingly avoiding formation of a coarse phase-separated structure that is prone to deteriorate glaze properties.

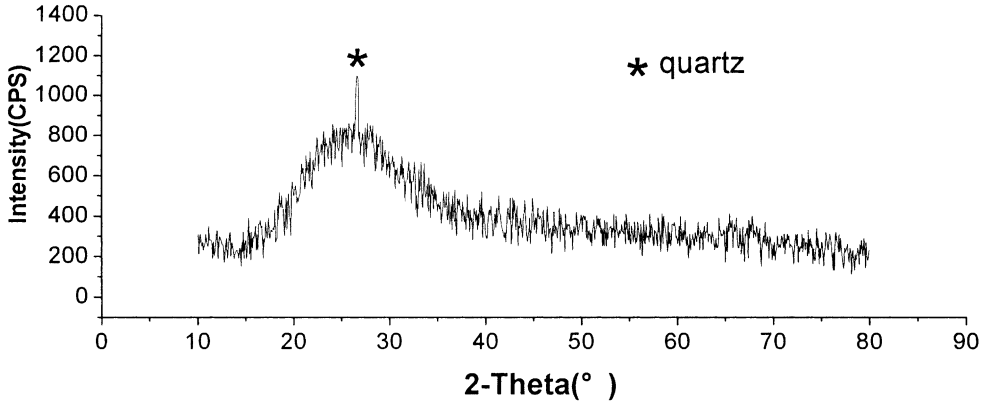

Fig. 1. XRD pattern of glaze Q6.

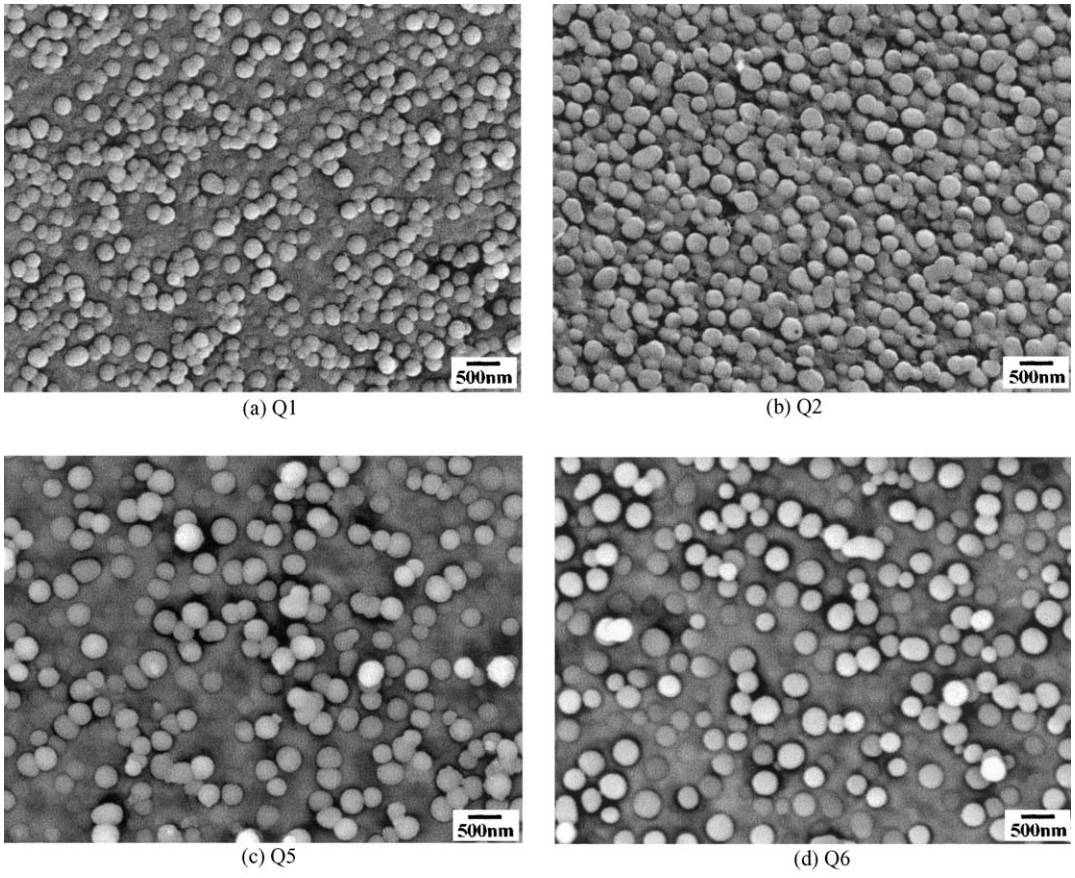

Fig. 2. FESEM images of glazes showing submicron droplet phase-separated structure.

After we incorporate the R_2O into K_2O, RO into CaO, and neglect the small amount of Fe_2O_3, TiO_2 and P_2O_5, the glaze compositions are roughly attributed to the quaternary system K_2O–CaO–Al_2O_3–SiO_2 which has a big phase separation volume [3] in which the liquid–liquid phase separation reaches a maximum with equimolar additions of alkali and alumina. As shown in Fig. 4, the six glaze compositions are situated close to the left side of the 1200 °C immiscibility boundary. The liquid–liquid immiscibility region should enlarge at lower than 1200 °C. Thus we could infer that the glazes bear thermodynamic qualifications for a phase-separated structure.

Chemical composition and thermal history are two key factors for the formation of appropriately scaled phase separation during a cooling cycle. The commonly used long hill-climbing dragon kiln in south of China meets the demands for a slow cooling rate which is essential for phase separation.

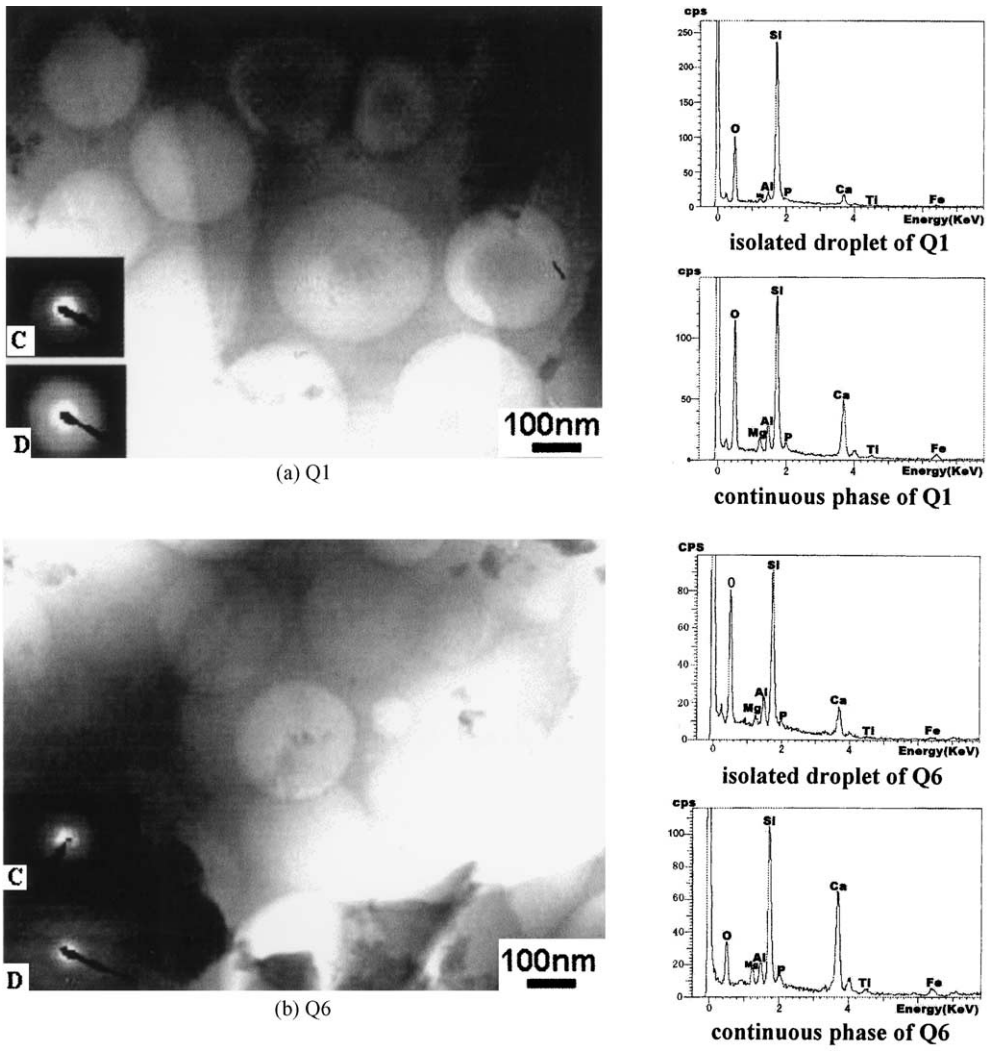

Fig. 3. TEM Images of glazes showing submicron droplet phase-separated structure, SAD images of(C) continuous phase and (D) droplet, indicating the feature of amorphous phase, EDS spectra showing compositional enrichment for the immiscible phases.

3.4. Determination of the immiscibility temperature

The immiscibility temperature is often defined as the temperature beyond which glass samples are transparent on quenching, whereas below this temperature they are opaque or reveal either opalescence or bluish tone. The refiring experiments were carried out with the shards. Firstly the samples were prepared by cutting off two pieces from each shard. Two groups of samples (six pieces in every group), numbered Q11–Q16 and Q21–Q26 were treated at 1250 °C for 2.5 h. Then Q11–Q16 were withdrawn from the furnace and thrown into cold water for rapid water cooling. Q21–Q26 remained in the muffle kiln, being cooled at a rate of 5 °C/min until 800 °C followed by power cut-off. Samples Q1–Q16 are clear and transparent and have been fired just right, indicating miscibility of the original separated phases. While Q21–Q26 have a jade-like opaque appearance, which means the phase separation leading to opacification develops during the slow cooling process. Then another experiment was performed in a gradient tube furnace on Q6 to further determine the immiscibility temperature. The sample was cut into fine strips of 4 mm wide, then the strips were aligned in a head-to-tail order into a ceramic boat. After that the boat was inserted into a gradient tube furnace in the temperature range 1220–800 °C. After holding for 2 h, the boat was withdrawn from the furnace for rapid water cooling, the turning position of the strips from being transparent to translucent is corresponding to the immiscibility temperature range, which is 1100–1150 °C from the experiment, according with the above conjecture in Fig. 4. As a result, we should anticipate liquid–liquid phase separation to occur during the cooling process.

3.5. Cause for opacification

For maximum scattering power, the second-phase particles should have an index of refraction far different from that of the matrix glass, they should have a particle

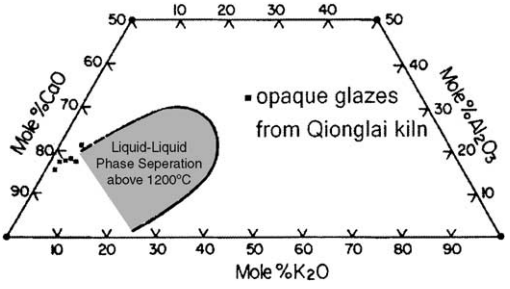

Fig. 4. Relation of glaze compositions to liquid-liquid phase separation region at 1200 °C on the (73.5±3.5) mol% SiO_2 plane of the K_2O–CaO–Al_2O_3–SiO_2 system by W.D. Kingery et al. [3].

size nearly the same as the wavelength of the incident visible light (0.39–0.77 μm), and the volume fraction of particles present should be high [4]. The glazes in this work consist of large volume of evenly dispersed submicron droplets separated from the matrices and they serve as the light scatters. Some droplets are conglomerative or junctural, enhancing light scattering. The equivalent diameter of the droplets falls in the range of 0.1–0.4 μm which is close to the wavelength range of the incident visible light, which causes intensive light scattering, thus resulting in good opacification, mild gloss and jade-like feel. Moreover, some bubbles which are several hundred microns in diameter and the little residue of quartz grains also make a minor contribution to the opacification of the glazes, but liquid–liquid phase immiscibility plays a key role in determining the charming artistic look.

The finding of phase-separated opaque glazes from Qionglai kiln site is another important find after the discovery of Tang dynasty phase separation glazes from Changsha and Wuzhou kiln sites. It is obvious that in the Tang dynasty, potters in different regions of China were already proficient in firing phase-separated opaque glazes, although they did not understand the inherent reasons at that time of over one thousand years ago. This study can provide a theoretical and technical basis for the development of a new group of opaque glazes or glasses.

4. Conclusion

The opaque green glaze from Qionglai Kiln Site is one of the earliest phase-separated opaque glazes in China. The glazes are high-temperature calcia–magnesia–silicate glazes and typical of phase-separated glazes with a submicron droplet structure, the isolated droplets are rich in SiO_2 and the matrix is rich in oxides of Ca, Mg, F, Ti and Fe. The discovery of the opaque green phase-separated glazes from Qionglai kiln site of the Tang dynasty revealed that the technique of utilizing liquid–liquid phase immiscibility to achieve a charming appearance of mild gloss and jade-like feel had been well developed as early as the Tang dynasty, which is of great significance to the development of the ceramic production in China.

References

1 F.-K. Zhang, Study on Qionglai kiln, in: '89 Science and Technology of Ancient Ceramics 1 Proceedings of the International Symposium, Shanghai Science and Technology Literature Publishing Company, Shanghai, 1989, pp. 50–53.
2 L.-Q. Chen, Study on Ancient Ceramics, Chongqing Publishing Company, Chongqing, 2001.
3 W.D. Kingery, P.B. Vandiver, L.-W. Huang, Y.-M Chiang, Liquid–liquid immiscibility and phase separation in the quaternary systems K_2O–Al_2O_3–CaO–SiO_4 and Na_2O–Al_2O_3–CaO–SiO_4, J. Non-Cryst. Solid 54 (1) (1983) 163–171.
4 O.V. Mazurin, E.A. Porai-Koshits, Phase Separation in Glass, North-Holland Physics Publishing, Netherlands, 1984.